

Article

Influence of the Phosphor Layer Composition on Flexible Electroluminescent Device Performance

Dina Esteves^{1,2,*}, Esra Akgül³ , Usha Kiran Sanivada^{1,2,4} , Inês P. Moreira^{1,2}, João Bessa^{1,2} , Carla A. Silva⁵, Fernando Cunha^{1,2,*} and Raul Fangueiro^{1,2}

¹ Fibrenamics—Institute for Innovation in Fiber-Based Materials and Composites, University of Minho, Campus de Azurém, 4800-058 Guimarães, Portugal; ushakiran.sanivada@gmail.com (U.K.S.)

² Center for Science and Technology (2C2T), University of Minho, Azurém Campus, 4800-058 Guimarães, Portugal

³ Department of Industrial Design Engineering, Faculty of Engineering, Erciyes University, 38090 Kayseri, Türkiye; akgul@erciyes.edu.tr

⁴ Department of Mechanical Engineering, University of Minho, Azurém Campus, 4800-058 Guimarães, Portugal

⁵ Simoldes Plastics, Research & Innovation, Rua Comendador António da Silva Rodrigues 165, 3720-052 Oliveira de Azeméis, Portugal

* Correspondence: dinaesteves81@gmail.com (D.E.); fernandocunha@fibrenamics.com (F.C.); Tel.: +351-964-471-987 (D.E.)

Abstract: Electroluminescence (EL) is an innovative technology in the lighting area. EL devices' main structure consists of a phosphor layer sandwiched between two electrodes. In this work, several alternating-current EL devices were developed by applying a set of sequential layers with combinations of in-house prepared inks and a commercially available ink as the phosphor layer. A flexible polyester textile substrate was functionalized with the inks by spray coating, after knife coating an interfacial layer directly on the surface. A thorough study was carried out on the phosphor layer composition to optimize the EL device performance, more precisely, illuminance intensity and illuminance homogeneity. The developed phosphor layer was composed of zinc sulfide doped with copper (between 30.0 and 38.1 wt%) and diluted by using a diluent at different concentrations (from 28.0 to 35.5 wt%). The best peak illuminance intensity of 61 lux was obtained when the phosphor ink presented a 35.4% ZnS:Cu ratio and was diluted with 33.0% diluent. This study aimed to determine the best formulation of the phosphor layer, which can be highly useful for further developments of EL devices, taking into account different applications in the market.

Keywords: electroluminescent textile; light-emitting textile; spray coating; phosphor layer



Citation: Esteves, D.; Akgül, E.; Sanivada, U.K.; Moreira, I.P.; Bessa, J.; Silva, C.A.; Cunha, F.; Fangueiro, R. Influence of the Phosphor Layer Composition on Flexible Electroluminescent Device Performance. *Coatings* **2024**, *14*, 554. <https://doi.org/10.3390/coatings14050554>

Academic Editor: Laura Sironi

Received: 21 March 2024

Revised: 24 April 2024

Accepted: 26 April 2024

Published: 30 April 2024



Copyright: © 2024 by the authors. Licensee MDPI, Basel, Switzerland. This article is an open access article distributed under the terms and conditions of the Creative Commons Attribution (CC BY) license (<https://creativecommons.org/licenses/by/4.0/>).

1. Introduction

Over the past few years, the automotive industry has been working on improving the lighting technology to enhance the user experience in the passenger compartment. The development of lighting solutions has been driven by several goals such as the achievement of increased brightness, longer lifetime, low cost, lightweight, and efficient devices that would use more environmentally sustainable materials. In this context, alternating-current powder electroluminescent (ACPEL) devices have emerged as a promising option due to their versatility and low power consumption.

Electroluminescence can be defined as “the phenomenon whereby light is emitted from a material following the application of an electric field to it” [1].

One of the significant milestones in the development of electroluminescence was the discovery of the phenomenon in 1936. The French physicist Georges Destriau discovered the phenomenon of ACP electroluminescence by observing luminescence from a suspension of ZnS:Cu phosphors in castor oil under a high electric field. ACPEL systems, in early studies, were found to be impractical and unsuitable for practical use due to their

insufficient illuminance and stability, as well as their inadequate lifetime, which was of only several hundred hours. The practical application of electroluminescent materials began in the 1960s with the development of EL displays and lighting devices and currently presents a high commercial potential [1,2]. Significant advancements were made in ACPEL in the 1990s by completely eliminating moisture-induced phosphor degradation, which has led to remarkable improvements in the lifespan of these devices [3].

From a general point of view, an ACPEL device has a specific structure consisting of a dielectric layer, a phosphor layer, and two electrode layers sandwiching the first two layers. When integrated into textiles, EL devices offer a unique combination of flexibility, durability, and aesthetics, making them suitable for various applications such as fashion wear, safety gear, and functional clothing. A wide range of materials can be used to fabricate EL textiles, including phosphorescent compounds, conductive polymers, and flexible substrates.

To functionalize textile substrates in the most effective way, it is imperative to apply an interface layer between the polyester surface and the back electrode layer. This crucial step prevents ink absorption by the textile surface, thereby enhancing the functionalization process.

Figure 1 shows the designed structure made during the experimental tests [4]. Each layer has a specific function, namely:

- The back electrode is a highly conductive, low-resistance layer in direct contact with the substrate surface or interface layer, ensuring efficient current flow;
- The busbar is a conductive layer that must be applied to the extremities to provide an optimal path for current distribution. This leads to maximum illuminance, making it a crucial element that should not be overlooked;
- The dielectric layer is an excellent electrical insulator that polarizes when exposed to an electric field. This polarization results in a highly conductive environment for light emission;
- Phosphor is a luminescent material responsible for light emission when excited by an electric field.
- The front electrode is a translucent conductive material that allows the electrical current to be evenly distributed, resulting in a uniform light output.

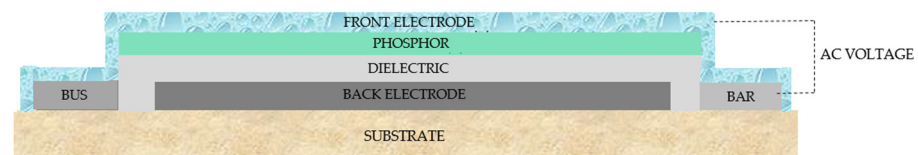


Figure 1. Schematic cross section of the electroluminescent structure.

Several studies were conducted in recent years on ACPEL textiles using various light-emitting materials and methods. Dumitrescu et al. explored the properties and potential of electroluminescent inks for textile substrates to create intricate surface patterns [5]. Similar works were found in the literature more recently. Ying Zhang et al. discussed the growing interest in textile-based flexible alternating-current electroluminescent devices, which have great potential in areas such as illumination, displays, smart wear, visual sensing, trendy decoration, and information interaction. However, despite their potential, there are still challenges in creating highly efficient EL devices that can deliver exceptional brightness and durability [6–8].

Ying Zhang et al. described a flexible electroluminescent device based on a ZnS:Cu/polyurethane composite and silver nanowires that was developed through a simple spin-coating method, layer by layer. To improve the polymer dielectric constant, BaTiO₃ was found to be the best filler. The electroluminescent performance of this device was explored in detail by studying the relationships between applied voltage, voltage frequency, and brightness [9].

As mentioned previously, the ACPEL structure comprises a thick emissive layer, known as a phosphor, typically measuring a few micrometers in thickness. The phosphor layer in an EL device plays a crucial role in the generation of light, essentially, in converting electrical energy into visible light through a process known as electroluminescence. When an electrical voltage is applied across the electrodes, it generates an electric field within the layer of zinc sulfide phosphor. This electric field stimulates the phosphor material and causes it to emit light. By adjusting the composition of the phosphor material and the voltage applied, the color of the light emitted can be controlled. The phosphor layer contains zinc sulfide (ZnS), an inorganic compound that emits light in an alternating-current electric field. The process of adding metallic elements, also known as doping, to ZnS phosphor crystals produces various colors of light, including yellow-orange, blue-green, blue, violet, pink, or white. The blueish-green luminescent color, in this case, was achieved by adding copper and aluminum to ZnS. The copper dopant metal within the phosphor crystals focuses the electrostatic field, which enables spontaneous emission to occur. The light emitted from the surface will have the same blueish-green color as the copper dopant and can be seen by the human eye. In summary, in a typical ACPEL device, a layer of phosphor and a layer of dielectric material are sandwiched between two conducting electrodes. When an AC voltage is applied across the two electrodes, the phosphor layer, more precisely the ZnS:Cu and Al particles emit blue-green light, visible to the human eye. To achieve a bright emission, transparent electrodes are used, namely the front electrode [10–18].

This study aimed to investigate the properties of the phosphor layer of ACPEL devices when applied on a polyester textile substrate using the spray coating technique. The spray coating method is a versatile choice for many electroluminescence applications that can be applied to various substrates, including flexible ones. This makes it possible to design and apply electroluminescent devices in different ways. The spray coating method is cost-effective compared to other coating methods, especially for large-scale production, since it reduces material waste and processing time. By adjusting the spray pressure, distance, and nozzle size, precise control over the coating thickness can be achieved.

The specific objective of this study was to determine the impact of altering the ZnS:Cu and diluent ratios on the composition of all structural phosphor layers that were deposited through the spray coating method. The main samples were analyzed in terms of ACPEL device performance, including illuminance intensity and homogeneity. Finally, the study presents the obtained optimized formulations. Additionally, one sample was prepared to explore the possibility of applying inks onto a rigid substrate made of PC/ABS to gain a better understanding of how the substrate type influences the outcome. However, the detailed investigation on producing ACPEL devices on rigid polymer surfaces is reserved for the future, based on the results obtained.

Section 1 described the advances in smart textiles that are used as part of lighting in the automotive sector, in particular, the fundamental research on EL properties of the phosphor layer by varying its formulation. In the Section 2, information related to the materials' characteristics is presented, and the method is described. Section 3 presents the outcomes of the results of the EL textile analysis. In Section 4, a summary of the research is presented, and the findings of this study are discussed and interpreted. Finally, in Section 5, the main conclusions of this study are presented.

2. Materials and Methods

2.1. Materials

To fabricate electroluminescent samples on a supporting polyester, an interface layer was coated first, followed by a sequential set of different layers, as depicted in Figure 1. Polyester (PES) was a fabric with a weight of 75 g/m², presenting a rectangular shape with dimensions of 7 × 12 cm. A commercial polycarbonate (PC)/acrylonitrile–butadiene–styrene (ABS) rectangular plaque was used as a control sample, with standard dimensions of 7 × 12 cm.

For the preparation of the inks and pastes, different polymers, namely, thermoplastic polyurethane (TPU) pellets, an acrylic liquid base, a conductive polymer, Clevios FE T, and, finally, a conductive polymer named polypyrrole (PPy), were used. Three different solvents, namely, *N,N*-dimethylformamide (DMF), tetrahydrofuran (THF), and a diluent (00527 PC thinner) were investigated. Specific compounds were used for the preparation of each functional layer: silver nanoparticles and multi-layer graphene platelets as conductive particles, barium titanate (BaTiO_3), an inorganic chemical compound which is available as a white powder for the dielectric layer, and, finally, luminescent particles for the phosphor layer.

Regarding the preparation of the interface layer, TPU pellets (Apilon 52[®] MA-6505, SpecialChem SA, Mussolente, Italy) were purchased; DMF (anhydrous, 99.8%) was purchased from Sigma-Aldrich (St. Louis, MO, USA), and THF (analytical-reagent grade, $\geq 99.8\%$) was purchased from Fisher Chemical (Hampton, NH, USA). This interface layer was applied by direct contact to the polyester substrates, by the knife coating technique, using the automatic film applicator coater ZAA 2300, purchased from Zehntner GmbH Testing Instruments, Sissach, Switzerland.

For the electroluminescent device structure, the coating technique adopted was spray coating. For that, a spray gun was obtained from Stardust (HVLP Spray Gun Kit, 4001, Stardust Colors SAS, St Laurent des Arbres, France). A nozzle with a diameter of 0.8 mm, an air pressure of 1.38–1.72 bar, and a distance of 20–25 cm between the substrate and the spray gun was used. To prevent the harmful evaporation of the solvents, a painting cabin and fume hood were used during the ink deposition process.

In order to create the ACEL device structure, the first layer, which was the conductive bottom electrode, was applied to the central area of the sample surface. In the second phase, the busbar was coated around the illuminated area to provide a low resistance path for a better current distribution. However, it is important to note that a short circuit can occur if the back electrode and the busbar come into contact with each other within the ACEL structure. To prevent this, it is crucial to carefully consider the minimum distance between these two elements during the coating process. In this specific case, the recommended distance was approximately 4 mm.

For the preparation of the back electrode and busbar formulations, the first layers to be applied directly on the surface by spray coating, a semi-matt acrylic lacquer with direct adhesion on plastic was purchased from Lechler, Como, Italy, more precisely, an acrylic base (LS947 2K plastic grip), a hardener (29355 Lechsys Acritop standard hardener), and a diluent (00527 PC thinner). Silver nanoparticles, 35 nm, 99.5%, NM-0023-HP (IoLiTec-Ionic Liquids Technologies GmbH, from Heilbronn, Germany), multi-layer graphene platelets PR0953 (Thomas Swan & Co. Ltd., Consett, UK), and a conductive-polymer, polypyrrole-doped 5 wt% dispersion in H_2O (Sigma Aldrich, St. Louis, MO, USA) were also used in different concentrations.

Regarding the insulating layer with a high dielectric constant, the same acrylic base, hardener, and diluent (Lechler, from Como, Italy) were used, and finally, barium titanate in powder, BT-301, was purchased (from WuXi Noble Electronics Co. Ltd., Wuxi, China).

For the phosphor layer, the base was the same; more precisely, the acrylic base, the hardener, the diluent (Lechler, Como, from Italy), and the luminescent particles, LP-6844, were provided by LWB-Leuchtstoffwerk Breitung GmbH, Breitung/Werra, Germany. Regarding the commercial phosphor layer, a standard ink was acquired from Lumilor company (Medina, OH, USA), more precisely, LC-B311-GR-Lumigreen, in order to produce a control sample. Finally, the top electrode layer, a translucent material allowing for light passage, consisted of the same solvents used in the interface layer, more precisely, DMF (anhydrous, 99.8%), purchased from Sigma-Aldrich (St. Louis, MO, USA), THF (analytical-reagent grade, $\geq 99.8\%$), provided by Fisher Chemical (Hampton, NH, USA), and the conductive polymer Clevios FE T, purchased from Heraeus Deutschland GmbH & Co., KG (Hanau, Germany).

The phosphor layer was prepared with varying ZnS:Cu ratios, ranging from 30.0 to 38.1 wt%, and with different amounts of diluent, between 28.0 and 35.5 wt%, as shown

in Table 1 below. The rest of the formulation consisted of the acrylic base and the hardener. Each specific formulation was then stirred magnetically for twenty minutes until a homogeneous solution was achieved.

Table 1. Matrix plan of the experiments.

Sample	Substrate	Phosphor Ink Composition	
		ZnS:Cu (wt%)	Diluent (wt%)
S1	Rigid PC/ABS	32.7%	30.5%
S2	Flexible PES	32.7%	30.5%
S3	Flexible PES	LC-B311-GR-Lumigreen *	
S4	Flexible PES	30.0%	30.5%
S5	Flexible PES	35.4%	30.5%
S6	Flexible PES	38.1%	30.5%
S7	Flexible PES	30.0%	28.0%
S8	Flexible PES	35.4%	33.0%
S9	Flexible PES	38.1%	35.5%

* Commercial phosphor ink, supplied by Lumilor company.

2.2. Methods

After determining the matrix plan for the experiments, we defined the key procedures for creating the formulations and constructing the electroluminescent device, as outlined below. In Figure 2, the primary steps for developing the phosphor ink formulation, before coating, can be observed.

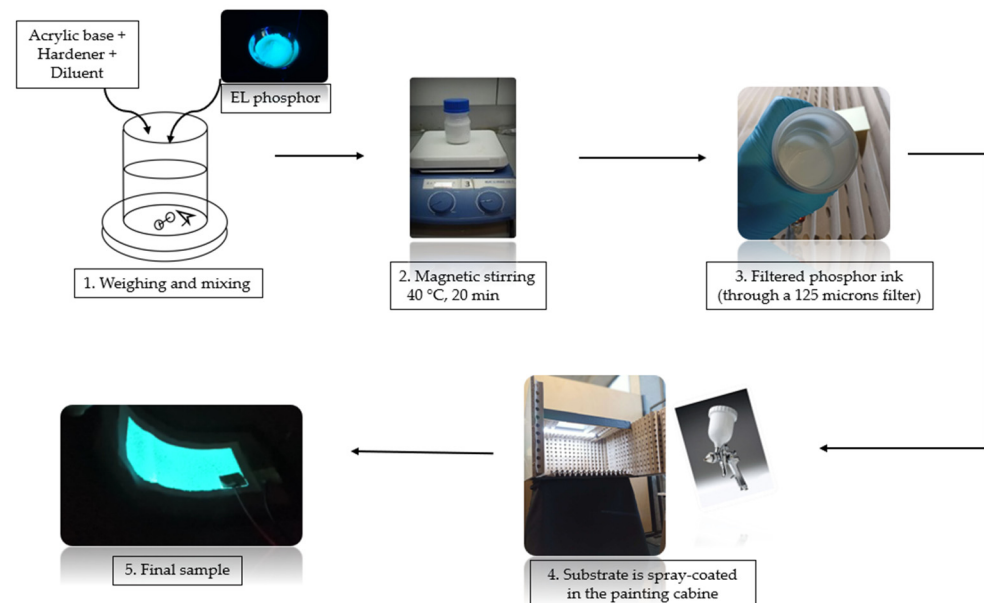


Figure 2. Schematic setup for the preparation of the phosphor ink.

Creating an electroluminescent device is a scalable process that requires following the main steps accurately. The main phases in building the electroluminescent device can be observed below, in Figure 3.

The composition of the phosphor layer used for the development of each EL device was analyzed in terms of sample morphology, chemical composition, and illuminance performance.

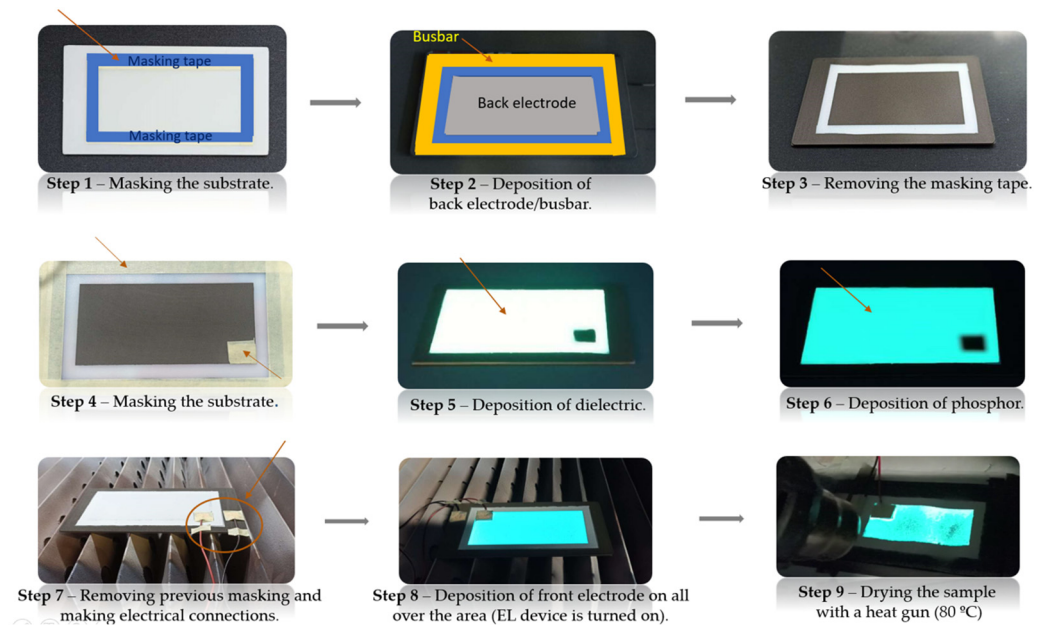


Figure 3. Main steps in the fabrication of the spray-coated electroluminescent device.

The morphological analyses were performed with the ultra-high-resolution field-emission-gun scanning electron microscope (FEG-SEM) NOVA 200 Nano SEM, FEI Company (Hillsboro, OR, USA). Topographic images were obtained with a secondary electron detector at an acceleration voltage of 10 kV. Before the analysis, the morphological analyses samples were covered with a thin film (35 nm) of Au-Pd (80–20 wt%) in the high-resolution sputter coater 208HR, from Cressington Scientific Instruments (Watford, UK), coupled to the MTM-20 Cressington High-Resolution Thickness Controller. The chemical analyses of the samples were performed by Energy-Dispersive Spectroscopy (EDS), using an EDAX Si (Li) detector (Hillsboro, OR, USA) at an acceleration voltage of 15 kV.

The illuminance values of the final functionalized substrates were measured with a light meter LT300 model (Extech Instruments, Nashua, NH, USA), up to 400,000 lux, with a high resolution of 0.01 Fc/lux, as shown below in Figure 4a. An average of three readings for each point was performed for each 9–12 standard spread points on the substrate surface, as shown below in Figure 4b.



(a) Digital light meter LT300.



(b) Measurement of illuminance.

Figure 4. (a) Digital light meter; (b) measurement of illuminance at different points of a functionalized surface.

Finally, regarding the functionalized polyester substrates, the thickness of each EL layer was measured using a Mitutoyo 2046F dial indicator, purchased from Mitutoyo Europe (Neuss, Germany).

3. Results

In this research, a set of electroluminescent inks were developed for application onto textile surfaces. The inks, with varying phosphor ratios, were applied to the textile surface using the spray coating technique, as shown in Figures 2 and 3. Following the application process, various performance and analytical tests were carried out. The resulting coated electroluminescent textile structures were fully functional and capable of emitting bluish-green ambient light.

3.1. Characterization by Scanning Electron Microscopy

SEM images were taken to examine the microstructures formed within the phosphor layer coated on PC/ABS without the interface layer (S1) and on the polyester substrates with the interface layer (S2, S3, S4, and S9). These microstructures are visible in the cross-section images (Figure 5a,c,e,g,i) as well as in the top view images (Figure 5b,d,f,h,j).

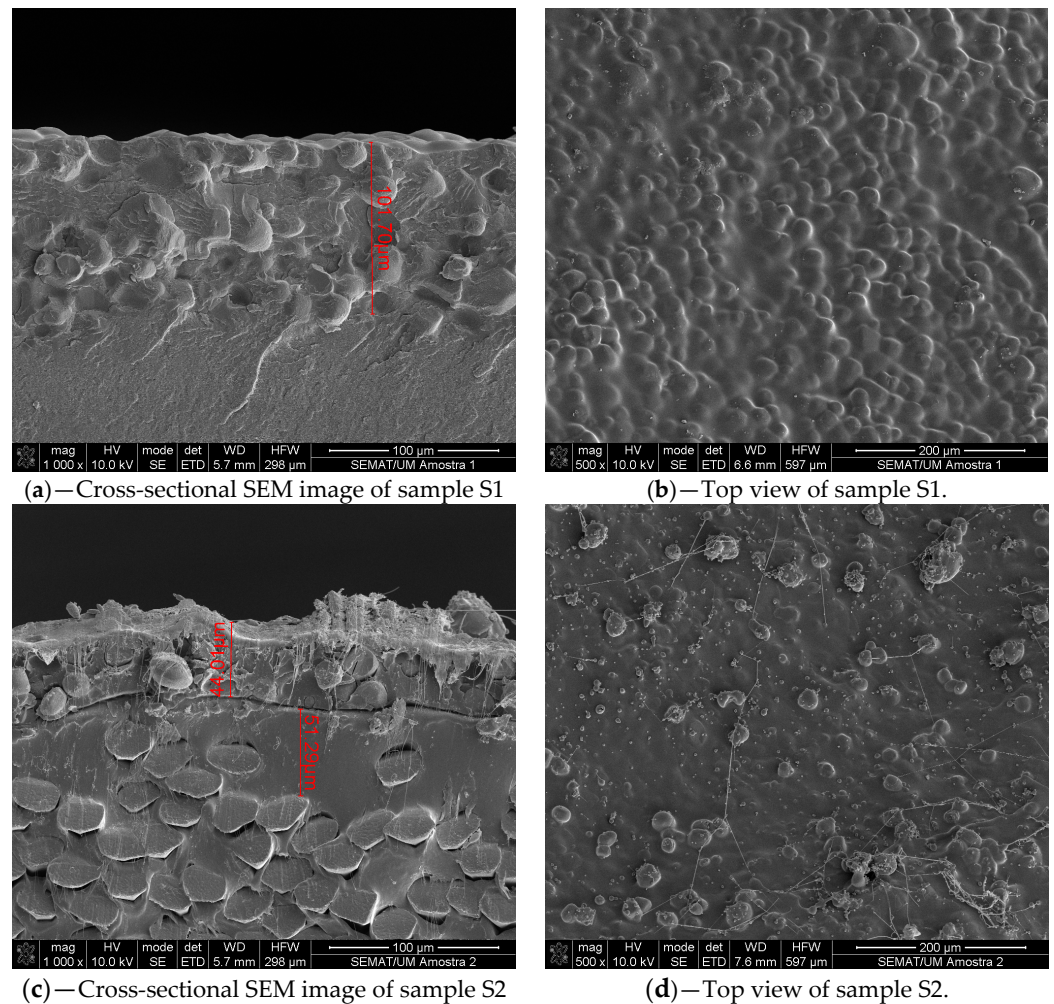


Figure 5. Cont.

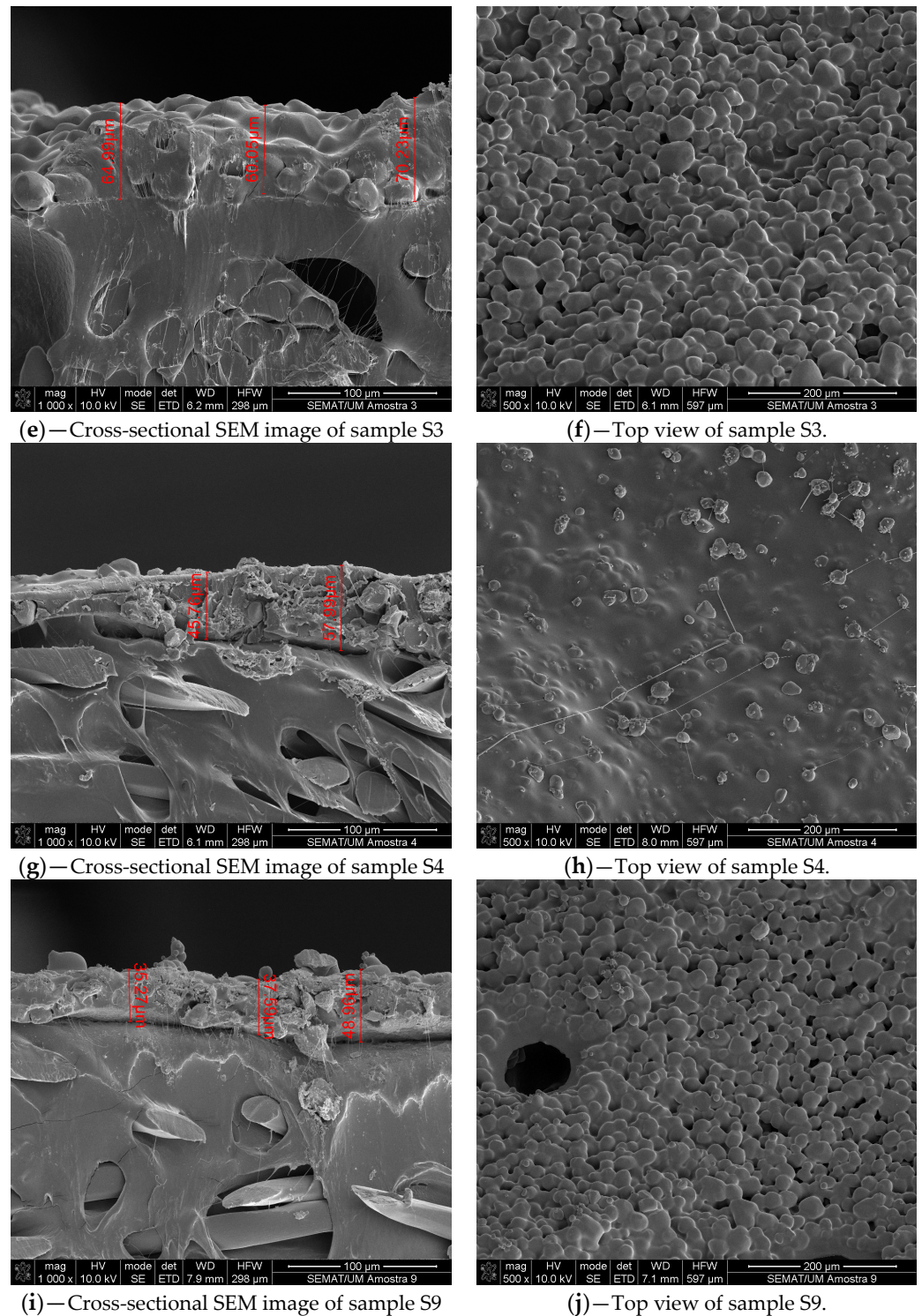


Figure 5. (a) Cross-sectional SEM image of the phosphor layer (32.7 wt% ZnS:Cu/30.5 wt% diluent) coated on the rigid PC/ABS substrate (S1); (b) Top view of the coating of the phosphor layer (32.7 wt% ZnS:Cu/30.5 wt% diluent) for the sample S1; (c) Cross-sectional SEM image of the phosphor layer (32.7 wt% ZnS:Cu/30.5 wt% diluent) coated on the interface layer of the polyester substrate (S2); (d) Top view of the coating of the phosphor layer (32.7 wt% ZnS:Cu/30.5 wt% diluent) for the sample S2; (e) Cross-sectional SEM image of the phosphor layer (LC-B311-GR-Lumigreen) coated on the interface layer of the polyester substrate (S3); (f) Top view of the coating of the phosphor layer (LC-B311-GR-Lumigreen) for the sample S3; (g) Cross-sectional SEM image of the phosphor layer (30.0 wt% ZnS:Cu/30.5 wt% diluent) coated on the interface layer of the polyester substrate (S4); (h) Top

view of the coating of the phosphor layer (30.0 wt% ZnS:Cu/30.5 wt% diluent) for the sample S4; (i) Cross-sectional SEM image of the phosphor layer (38.1 wt% ZnS:Cu/35.5 wt% diluent) coated on the interface layer of the polyester substrate (S9); (j) Top view of the coating of the phosphor layer (38.1 wt% ZnS:Cu/35.5 wt% diluent) for the sample S9.

The SEM images in Figure 5 provide clear evidence of the coating thickness and distribution of phosphor particles on both the PC/ABS substrate and the fabric surface. The cross-sectional SEM image of the first sample S1 (Figure 5a) conclusively demonstrates a uniform coating thickness of approximately 101.7 μm , which was attributed to the rigidity and non-porosity of the polymeric surface. Additionally, the SEM image in Figure 5b shows a uniform distribution of the phosphor particles, resulting in a homogeneous surface layer on the substrate.

In contrast, the SEM image of the second sample S2 (Figure 5c) demonstrates a lower thickness of the phosphor layer (about 48.0 μm) and a higher variation in the coating thickness. This difference was caused by the higher porosity of the fabric surface, which allowed for the penetration and absorption of the phosphor ink. It is important to note that the same formulation of the phosphor layer was used for both samples, but sample S1 comprised a rigid PC/ABS substrate. In Figure 5d, the SEM surface image displays the top of the phosphor layer applied on the polyester substrate, which showcases an uneven distribution of the phosphor particles. This resulted in a heterogeneous surface compared to that observed when the phosphor layer was coated on PC/ABS, which displayed a homogeneous distribution of the particles.

The cross-sectional SEM image presented in Figure 5e clearly shows the thickness of the commercial phosphor layer to be approximately 76.0 μm . The coating thickness varied due to the roughness of the polyester textile. Notice the entirely uniform surface of the commercial phosphor sample illustrated in Figure 5f.

The SEM image in Figure 5g indicates that the thickness of the phosphor layer was approximately 51.9 μm . In this case, the thickness was a critical factor in achieving the desired outcome, and it is evident that it was not uniform. In Figure 5h, it is apparent that the ZnS:Cu particles were not well dispersed on the surface of the layer for sample S4, which contained 30.0 wt% ZnS:Cu and 30.5 wt% diluent.

Concerning Figure 5i, it is noticeable that there was a certain level of uniformity concerning the thickness, which, more precisely, was 40.6 μm . The SEM image in Figure 5j unambiguously confirms the formation of a homogeneous surface layer on the substrate due to the uniform distribution of the phosphor particles. In this view from above related to Figure 5j, it is possible to observe several empty spaces on the coated surface due to the excess of ZnS:Cu particles that were not well dispersed in the phosphor formulation. For this sample S9, this formulation contains a ratio of 38.1% ZnS:Cu and 35.5% diluent.

3.2. Illuminance Measurements

The ACPEL devices emitted bluish-green light, as demonstrated in Figure 6. To determine the level of illuminance homogeneity, all samples underwent rigorous investigation at various points on the surface, using a light meter. These measurements were acquired by applying a 12 V DC voltage as a power source, which was then converted into AC voltage through an inverter. It is worth noting that an EL device must generate a constant AC voltage of 150 V at an average frequency of 2.68 KHz to function properly [12].

3.2.1. Performance Evaluation of the Samples

The homogeneity factor is calculated using Equation (1), by calculating the percentual ratio between the standard deviation and the average of the illuminance values. This calculation provides information about the variability of the illuminance values. A higher value, up to a maximum of 100%, indicates greater uniformity of the light emitted by the functionalized surface.

$$HF = 100 - \left[\frac{\text{Standard deviation}}{\text{Average}} \times 100 \right] \quad (1)$$



Figure 6. ACPEL devices: (a) sample S1, functionalized on the PC/ABS substrate; (b) sample S2, functionalized on the polyester substrate.

In Figures 7–10, the relationship between the illuminance/homogeneity and the composition of the phosphor layer is shown; more precisely, the ZnS:Cu and diluent ratio change in the formulation. According to Figure 7, different concentrations of the ZnS:Cu powder (30.0, 32.7, 35.4, and 38.1 wt%) were dispersed in the acrylic base and hardener and, on the other hand, the diluent amounts were fixed at 30.5 wt%.

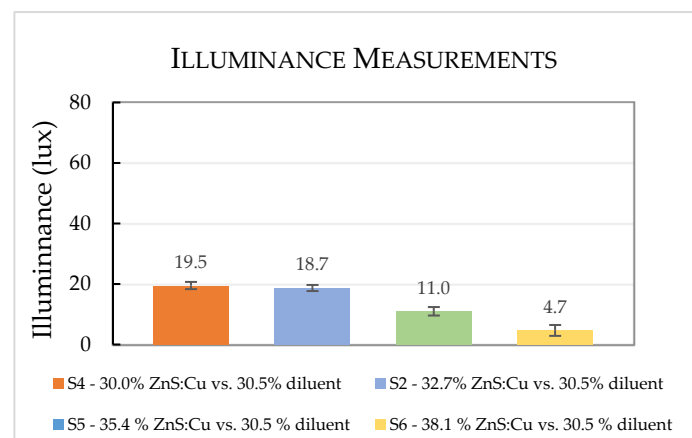


Figure 7. Illuminance measurements of samples S4, S2, S5, and S6, with increasing content of ZnS:Cu in the formulation.

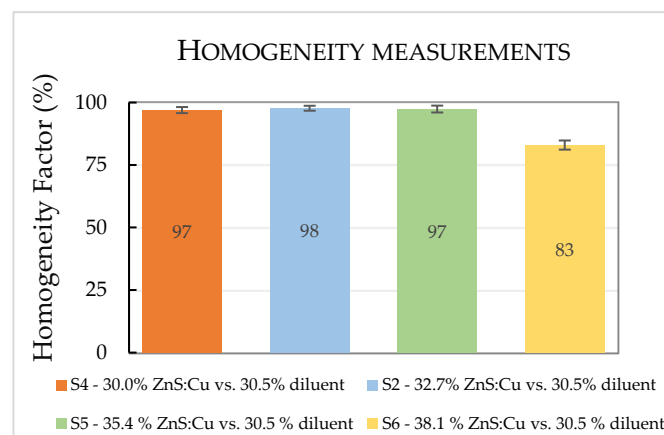


Figure 8. Homogeneity factor, calculated for samples S4, S2, S5, and S6.

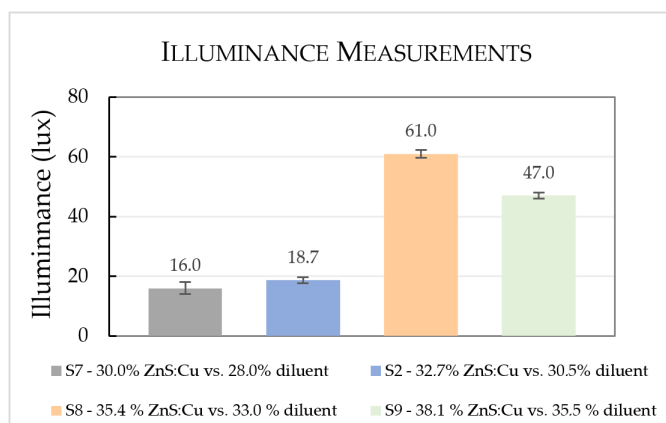


Figure 9. Illuminance measurements of samples S7, S2, S8, and S9, with increasing contents of ZnS:Cu and diluent.

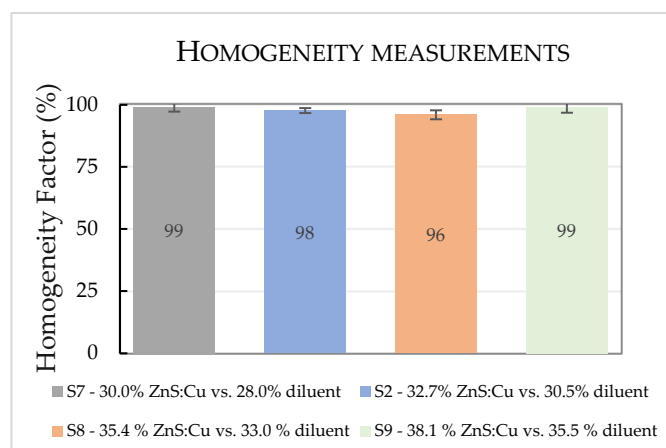


Figure 10. Homogeneity factor, calculated for samples S7, S2, S8, and S9.

Based on the results presented in Figures 7 and 9, sample 8 showed the highest illuminance values of 61 lux, achieved with 35.4 wt% of ZnS:Cu and 33.0 wt% of diluent, using an applied AC voltage of 150 V. This sample performed better than sample S5, which had a similar formulation but only 30.5 wt% of diluent. This observation suggests that increasing the quantity of diluent by 2.5 wt% in the formulation could lead to larger values of illuminance. The high illuminance values of the functionalized textile substrates were attributed to the phosphor formulations, which were prepared by adding a ZnS:Cu ratio between 35.4 wt% and 38.1 wt% and a diluent ratio between 33.0 wt% and 35.5 wt%.

After analyzing the data presented in Figures 8 and 10, it was found that the calculated homogeneity factor had high values, up to 96%. However, sample S6, with 38.1 wt% of ZnS:Cu and 30.5 wt% of diluent, had the lowest homogeneity factor.

3.2.2. Performance Evaluation of the Developed Samples

All developed samples were fully functional, and the peak illuminance intensity was undoubtedly achieved for the functionalized PC/ABS substrate, with a maximum average value of 97.5 lux, as clearly shown in Figure 11. However, it is noteworthy that this sample presented the lowest value of the homogeneity factor, corresponding to 82% only.

On the contrary, for the functionalized polyester substrate samples, increasing the percentages of ZnS:Cu and diluent in the formulation resulted in higher values of illuminance. The best value of illuminance of 61 lux and the best homogeneity factor of 96% were achieved for sample S8, indicating its superiority over the other samples.

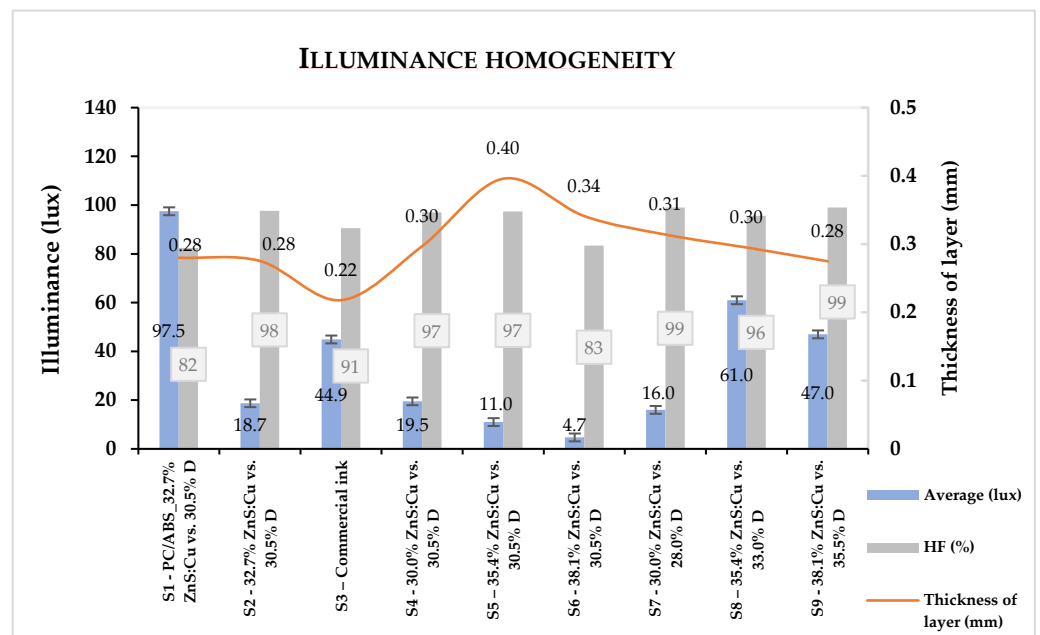


Figure 11. Illuminance/homogeneity factor and thickness measurements of all developed samples (samples S1 to S9).

For all the functionalized substrates, we analyzed the thickness of all layers in the EL device, including the back electrode, dielectric, phosphor, and front electrode layers, taking in account the light intensity performance for each ACEPL device, as depicted in Figure 11. Regarding the flexible textile-based ACEPL device, it is worth noting that all functional layers of the structure had a thickness greater than 0.22 mm and less than 0.40 mm. The illuminance measurements showed that the peak light intensity was achieved for samples S3, S8, shown below in Figure 12, and S9, which had thicknesses of the ACEPL devices of 0.22 mm, 0.30 mm, and 0.28 mm, respectively. This indicates that a thin layer in the ACEPL structure, with a specific thickness within the micrometer range, can be highly effective and represents an interesting low-cost approach for the automotive sector, among other industrial sectors [16].



Figure 12. Sample 8 (35.4% ZnS:Cu and 33% diluent).

Figure 13, shown below, presents SEM images that aid in comprehending the morphology of the coated layer for the specific phosphor ink with 35.4% ZnS:Cu/33% diluent, corresponding to sample S8.

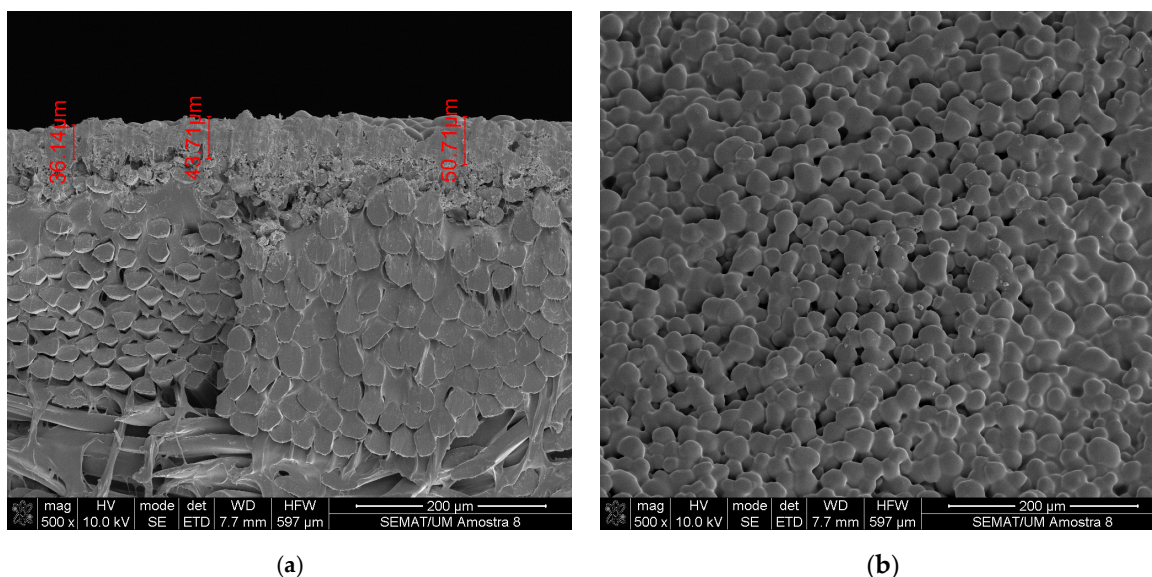


Figure 13. SEM images of sample 8: (a) cross section of the phosphor layer, scale bar: 100 μm ; (b) top of the phosphor layer, scale bar: 200 μm .

The scanning electron microscope (SEM) image of the cross section in Figure 13a reveals a varying coating thickness between 36.14 μm and 50.71 μm due to the roughness of the polyester textile. On the other hand, Figure 13b displays a uniform distribution of the phosphor particles on the surface of sample 8, thanks to the optimization of the ratios of ZnS:Cu and diluent in the sample composition [19].

To identify the chemical elements present in the coating used in this study, the Energy-Dispersive Spectroscopy (EDS) technique was employed. Several areas on the surface of sample 8 were selected randomly and analyzed using this technique. The results obtained are displayed in Table 2, presented below.

Table 2. Results of the EDS analysis of sample 8.

Element	wt%
C	53.05
O	4.77
Al	2.36
S	4.79
Zn	35.03
Total	100.00

The analysis of sample S8 provided a clear picture of the chemical composition of the sample. Carbon and zinc were found to be the primary chemical elements present, with zinc accounting for a significant 35.03%. While sulfur, oxygen, and aluminum were also identified, their presence was minimal. Of particular interest was the use of zinc sulfide doped with aluminum in the phosphor layer for electroluminescence. The luminescent particles LP-6844 used for the phosphor, mainly consist of zinc sulfide doped with copper and other residual metallic elements, such as aluminum. These elements work together to create a blueish-green color when sandwiched between two electrode layers. However, it is worth noting that the EDS analysis did not detect copper elements in this case due to the random character of this surface analysis.

3.2.3. Performance Evaluation during the Device's Lifetime

In the field of electroluminescence, the degradation of illuminance intensity is a crucial parameter when designing ACPEL applications. The longevity of a device is determined

by two factors: its “useful life” and its “half-life”. The “half-life” refers to the duration it takes for illuminance to decline to half of its original value while the electroluminescent device is continuously turned on. This value is measured in days and is influenced by the applied voltage and frequency [20].

Regarding the sample S1, Figure 14 shows an initial illuminance value of 98 lux. After 90 h of operation in the same power supply conditions (voltage of 155 Vac, at a frequency of 989 Hz), an average illuminance value of 90 lux was observed, which corresponded to an 8% drop in illuminance compared to the initial value, meaning that the half-life value of the sample was not reached after 90 h in continuous operation.

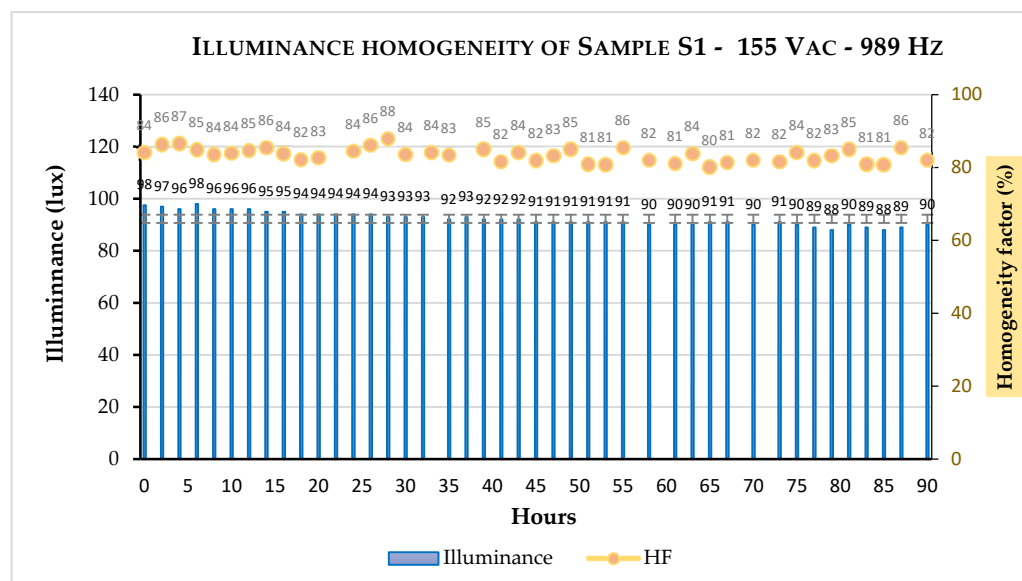


Figure 14. Performance evaluation during the device lifetime, for 90 h (for sample S1).

4. Discussion

We demonstrated that it is possible to fabricate flexible textile-based ACEPEL devices that can bend and conform to curved shapes. This was shown using the samples from 2 to 9. Additionally, we found that these devices worked equally well when fabricated on rigid polymer substrates (PC/ABS), as demonstrated by the first sample S1. This versatility in product design makes ACEPEL devices suitable for various applications in the automotive and other industries.

The production of a single sample (S1) using the PC/ABS substrate allowed us to investigate the possibility of producing similar devices using a rigid substrate. To explore these possibilities and understand the impact of the substrate on illuminance and homogeneity, we used the same formulation to produce ACEPEL devices while varying the substrate.

Our findings indicated that the ACEPEL device with a rigid substrate performed better than that with flexible PES. This could be attributed to differences in the performance of the functionalized substrates, despite using coated layers with the same ink composition, as observed in the case of samples S1 and S2. The flexible substrate with PES absorbed some of the coated inks because of the presence of voids, as shown in the SEM images of previous Figure 5. Hence, a detailed study can be made in the future considering these observations to understand the influence of the substrate and of the composition of the inks.

The presence of ZnS:Cu in the composition of the ink can have a vital influence on illuminance, and hence, various samples were produced with various ZnS:Cu concentrations, more precisely, varying between 35.4% and 38.1%, fixing the diluent ratio (30.5%). The results showed that the increasing concentration of ZnS:Cu resulted in a decrement in illuminance. As the diluent ratio was fixed at 30.5%, it was evident that the formulations did not contain enough diluent to enable the proper dispersion of the ZnS:Cu particles

in the formulations. Consequently, a decline in the illuminance values was observed in the samples S5 and S6. It was also understood that the sample S4 might have reached the optimized diluent ratio, which was nearly the same as the ZnS:Cu concentration.

This study aimed to investigate the impact of the diluent on the ink composition. To achieve this, samples were created by keeping the amount of ZnS:Cu in the composition constant and varying the diluent ratio. The results of the study are noteworthy. By increasing the diluent ratio, the illuminance value increased from 4.7 lux to 47.0 lux. This increase in the diluent ratio could be the reason for the proper dispersion of ZnS:Cu in the phosphor. The SEM images shown in Figures 5 and 13 further support this observation. Therefore, it can be inferred that nearly equal concentrations of ZnS:Cu and diluent were required to facilitate the proper distribution of ZnS:Cu, as observed in the case of sample S8 which includes a phosphor layer composition with a ratio of 35.4% of ZnS:Cu and a ratio of 33.0% of diluent.

These findings are highly significant and can have important implications for future research in this field [21,22].

As regards the SEM image analysis, it seems highly probable that the fabric partially absorbed the layered ink, despite being coated with a TPU-based interface layer. This was due to the presence of voids on the surface of the polyester fabric, which is porous. Through our research experiments, we discovered that the functional electroluminescent layers had an incredibly small total thickness, ranging between 0.22 and 0.40 mm. Therefore, it is crucial to avoid the excessive coating of a material that can negatively impact the performance of an EL device in terms of illuminance. On the other hand, using thinner layers can significantly reduce the final cost of the device, providing an economic benefit.

Regarding the device lifetime, some degradation in terms of illuminance intensity was observed after 90 h of continuous operation, under the same conditions of voltage, more precisely, a decrease of 8% of illuminance over time.

5. Conclusions

This study aimed to improve the lighting performance of textile surfaces by creating new formulations for each functional layer of the electroluminescent structure. The researchers used innovative formulations for the back electrode, busbar, dielectric, phosphor, and front electrode layers to develop EL textile devices. Specifically, we investigated the impact of different ZnS:Cu and diluent ratios on the composition of a specific and important layer, i.e., the phosphor layer.

The functionalized substrates were investigated to evaluate illuminance and homogeneity in different points of the sample surface, using a lux meter. Based on the analysis, the EL textile device corresponding to sample S8 displayed a higher illuminance value of 61 lux compared to the other samples.

This particular formulation contained a higher ratio of copper-doped zinc sulfide, specifically, 35.4 wt%, and an optimal diluent ratio of 33.0 wt%, which led to a better dispersion of the copper-doped zinc sulfide particles in the ink.

The results obtained from this research indicate that the innovative inks developed are functional and will enable the production of flexible electroluminescent (EL) devices. The stretchable display can be attached to curved surfaces, and these thin and flexible EL devices have great potential in various applications such as wearable electronic devices, ambient lighting in the automotive sector, and fashion design, among others. The presented approach aimed to reduce the basic weight and improve the structural efficiency, while also reducing the economic and environmental impact, in line with the sustainable development of materials.

Future studies will focus on a more detailed evaluation of the illuminance properties of flexible substrates as well as rigid substrates under environmental, mechanical, and aging factors to gain a better understanding of this innovative lighting technology. Proper encapsulation could protect the ACPEL devices from moisture, oxygen, and other environmental factors that can degrade the materials they contain over time. Hermetic sealing or

barrier films can help prolong a device's lifetime. By considering factors such as material selection and the optimization of the design and of the operational parameters may lead to further advancements to extend EL devices' lifetime.

Author Contributions: Conceptualization, D.E. and I.P.M.; methodology, D.E. and I.P.M.; validation, D.E., E.A. and I.P.M.; formal analysis, D.E. and I.P.M.; investigation, D.E., E.A. and C.A.S.; resources, J.B., F.C. and R.F.; data curation, D.E.; writing—original draft preparation, D.E. and I.P.M.; writing—review and editing, D.E., E.A., U.K.S. and I.P.M.; visualization, J.B.; supervision, J.B., F.C. and R.F.; project administration, F.C. and R.F.; funding acquisition, F.C. and R.F. All authors have read and agreed to the published version of the manuscript.

Funding: This research was funded by the European Regional Development Fund (ERDF) through the Portugal 2020 Competitive Factors Operational Program (POCI), Grant number POCI-01-0271-FEDER-049652 related to the project LH4Auto—Lighting and Heating System for Automotive, and project ProtechMask—New generation of active reusable masks for protection, code POCI-01-0247-FEDER-070021. The authors also acknowledge the support of the Portuguese Foundation for Science and Technology (FCT) for the strategic funding of UID/CTM/00264/2020 of 2C2T—Center for Textile Science and Technology.

Institutional Review Board Statement: Not applicable.

Informed Consent Statement: Not applicable.

Data Availability Statement: The raw data supporting the conclusions of this article will be made available by the authors on request.

Acknowledgments: The authors would like to acknowledge Fibrenamics—Institute of Innovation in Fiber-Based Materials and Composites and 2C2T from University of Minho. This article/publication is based upon work from the COST Action CA17107—European Network—to connect research and innovation efforts on advanced smart textiles, which was supported by COST (European Cooperation in Science and Technology) www.cost.eu (accessed on 22 November 2023).

Conflicts of Interest: The authors declare no conflict of interest.

References

1. Kathirgamanathan, P.; Bushby, L.M.; Kumaravel, M.; Ravichandran, S.; Surendrakumar, S. Electroluminescent Organic and Quantum Dot LEDs: The State of the Art. *J. Disp. Technol.* **2015**, *11*, 480–493. [[CrossRef](#)]
2. Fernández, M.R.; Casanova, E.Z.; Alonso, I.G. Review of Display Technologies Focusing on Power Consumption. *Sustainability* **2015**, *7*, 10854–10875. [[CrossRef](#)]
3. Zhang, X.; Wang, F. Recent advances in flexible alternating current electroluminescent devices. *APL Mater.* **2021**, *9*, 030701. [[CrossRef](#)]
4. Chansri, P.; Arunrungrusmi, S.; Yuji, T.; Mungkung, N. An Analysis of ZnS:Cu Phosphor Layer Thickness Influence on Electroluminescence Device Performances. *Int. J. Photoenergy* **2017**, *2017*, 4. [[CrossRef](#)]
5. Kooroshnia, M.; Dumitrescu, D.; Lewis, E.; Walters, K. The colour, texture, and luminance: Textile design methods for printing with electroluminescent inks. *Cult. Sci. Color.-Color Cult. Sci. J.* **2023**, *15*, 27–34.
6. Janczak, D.; Zych, M.; Raczyński, T.; Dybowska-Sarapuk, Ł.; Pełowski, A.; Krzemiński, J.; Sosna-Głębska, A.; Znajdek, K.; Sibiński, M.; Jakubowska, M. Stretchable and Washable Electroluminescent Display Screen-Printed on Textile. *Nanomaterials* **2019**, *9*, 1276. [[CrossRef](#)] [[PubMed](#)]
7. Graßmann, C.; Grethe, T.; Van Langenhove, L.; Schwarz-Pfeiffer, A. Digital printing of electroluminescent devices on textile substrates. *J. Eng. Fibers Fabr.* **2019**, *14*, 1558925019861624. [[CrossRef](#)]
8. Wang, L.; Xiao, L.; Gu, H.S.; Sun, H.D. Advances in Alternating Current Electroluminescent Devices. *Adv. Opt. Mater.* **2019**, *7*, 1801154. [[CrossRef](#)]
9. Zhang, Y.; Wang, X.; Zhang, Y.; Liu, M.; Zhao, Z.; Shen, Z.; Hu, Y. Wearable Alternating Current Electroluminescent e-Textiles with High Brightness Enabled by Fully Sprayed Layer-by-Layer Assembly. *Adv. Funct. Mater.* **2024**, *34*, 2308969. [[CrossRef](#)]
10. Verboven, I.; Deferme, W. Printing of flexible light emitting devices: A review on different technologies and devices, printing technologies and state-of-the-art applications and future prospects. *Prog. Mater. Sci.* **2020**, *118*, 100760. [[CrossRef](#)]
11. Hu, B.; Li, D.; Ala, O.; Manandhar, P.; Fan, Q.; Kasilingam, D.; Calvert, P.D. Textile-Based Flexible Electroluminescent Devices. *Adv. Funct. Mater.* **2011**, *21*, 305–311. [[CrossRef](#)]
12. Lumilor Basics and FAQ. Available online: <https://support.lumilor.com/lumilor/lumilor-basics-and-faq#properties-of-lumilor-3> (accessed on 22 January 2023).

13. Park, B.J.; Seo, H.S.; Ahn, J.T.; Song, J.H.; Chung, W.J.; Jeon, D.Y. An investigation on photoluminescence and AC powder electroluminescence of ZnS:Cu,Cl,Mn,Te phosphor. *J. Mater. Res.* **2011**, *26*, 2394–2399. [[CrossRef](#)]
14. Withnall, R.; Silver, J.; Harris, P.G.; Ireland, T.G.; Marsh, P.J. AC powder electroluminescent displays. *Soc. Inf. Disp. J.* **2011**, *19*, 798–810. [[CrossRef](#)]
15. Policia, R.; Correia, D.M.; Peřinka, N.; Tubio, C.R.; Lanceros-Méndez, S. Influence of polymer matrix on the luminescence of phosphor based printable electroluminescent materials and devices. *Polymer* **2023**, *268*, 125700. [[CrossRef](#)]
16. Fadavieslam, M.R. The effect of thickness of light emitting layer on physical properties of OLED devices. *Optik* **2019**, *182*, 452–457. [[CrossRef](#)]
17. Mi, H.; Zhong, L.; Tang, X.; Xu, P.; Liu, X.; Luo, T.; Jiang, X. Electroluminescent Fabric Woven by Ultrastretchable Fibers for Arbitrarily Controllable Pattern Display. *ACS Appl. Mater. Interfaces* **2021**, *13*, 11260–11267. [[CrossRef](#)]
18. Sloma, M.; Janczak, D.; Wroblewski, G.; Mlozniak, A.; Jakubowska, M. Electroluminescent structures printed on paper and textile elastic substrates. *Circuit World* **2014**, *40*, 13–16. [[CrossRef](#)]
19. Payne, S.; Moore, J. Preparation of Cross Sections of Difficult Materials for SEM Imaging. *Microsc. Today* **2018**, *26*, 40–45. [[CrossRef](#)]
20. Marques dos Anjos, P.N. Analysis of electroluminescence degradation for organic light-emitting diode using a rate equation of chemical kinetics. *J. Inf. Disp.* **2013**, *14*, 115–120. [[CrossRef](#)]
21. Bochkov, Y.V.; Georgobiani, A.N.; Chilaya, G.S. Electroluminescence and Some Electrical Properties of Homogeneous Zinc Sulfide Single Crystals. In *Electroluminescence/Elektrolyuminescenciya/Электрoлюминесценция*; The Lebedev Physics Institute Series; Springer: Boston, MA, USA, 1972; Volume 50. [[CrossRef](#)]
22. Lee, W.; Lyu, H.K.; Cho, H.S.; Lee, S.E.; Choi, B. Brightness enhancement of a direct-current-driven electroluminescent device prepared with zinc-sulfide powder. *J. Lumin.* **2020**, *220*, 117015. [[CrossRef](#)]

Disclaimer/Publisher’s Note: The statements, opinions and data contained in all publications are solely those of the individual author(s) and contributor(s) and not of MDPI and/or the editor(s). MDPI and/or the editor(s) disclaim responsibility for any injury to people or property resulting from any ideas, methods, instructions or products referred to in the content.